

Supporting Information

Stretchable Capacitive Fabric Electronic Skin Woven by Electrospun Nanofiber

Yarn for Detecting Tactile and Multimodal Mechanical Stimuli

Xiaolu You,^{ab} Jianxin He,^{*ab} Nan Nan,^{ab} Xianqiang Sun,^{ab} Kun Qi,^c Yuman Zhou,^c Weili Shao,^{ab} Fan Liu^{ab} and Shizhong Cui^{ab}

^a Henan Provincial Key Laboratory of Functional Textile Materials, Zhongyuan University of Technology, Zhengzhou 450007, China

^b Collaborative Innovation Center of Textile and Garment Industry, Henan Province, Zhengzhou 450007, China

^c School of Textile and Clothing, Jiangnan University, Wuxi 214122, China

***Corresponding author:** Jianxin He

P.O. Box 110, College of Textiles, Zhongyuan University of Technology, 41 Zhongyuan Road, Zhengzhou City 450007, Henan Province, People's Republic of China

E-mails: hejianxin771117@163.com



Figure S1 Digital image of the Ni-coated cotton yarns wound on a bobbin.

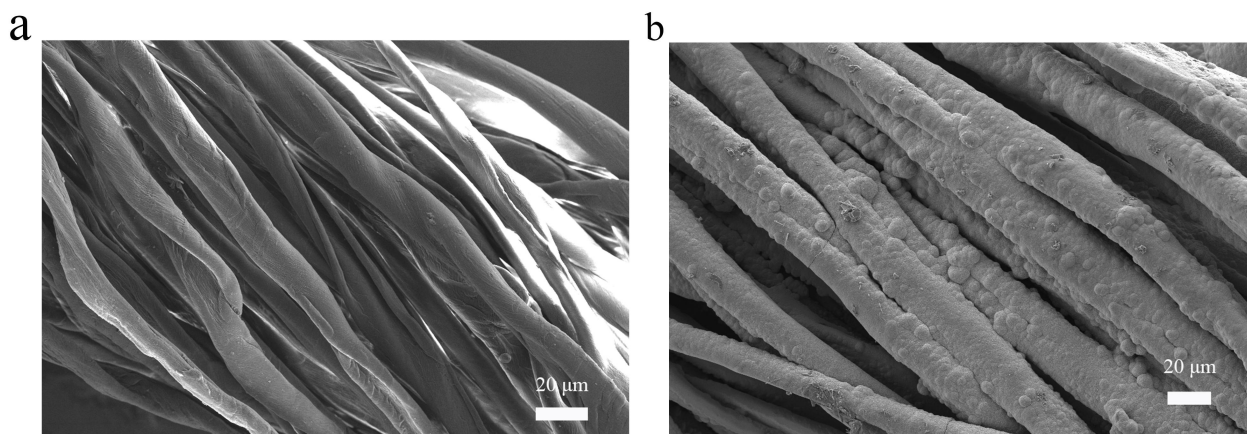


Figure S2 The same magnification SEM images of (a) pristine cotton yarn and (b) Ni-coated cotton yarn.

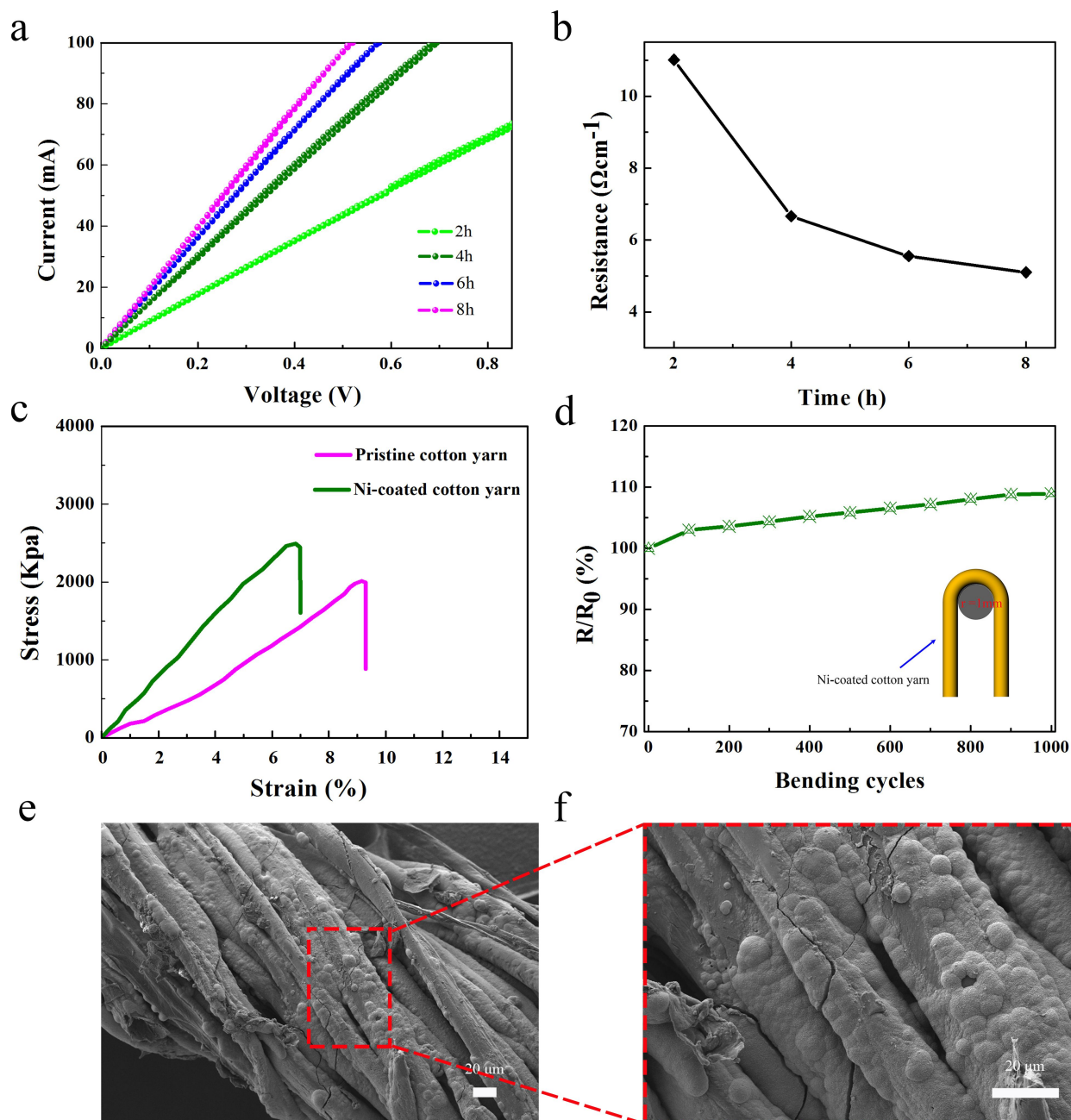


Figure S3 I-V curves (a) and electrical resistance (b) of the Ni-coated cotton yarn with different electroless deposition times (2, 4, 6, and 8h). (c) Stress-strain curves of pristine cotton yarn and Ni-coated cotton yarns. Electrical resistance (d) and SEM images (e, f) of Ni-coated cotton yarn after bending 1000 cycles (bending radius 1mm).

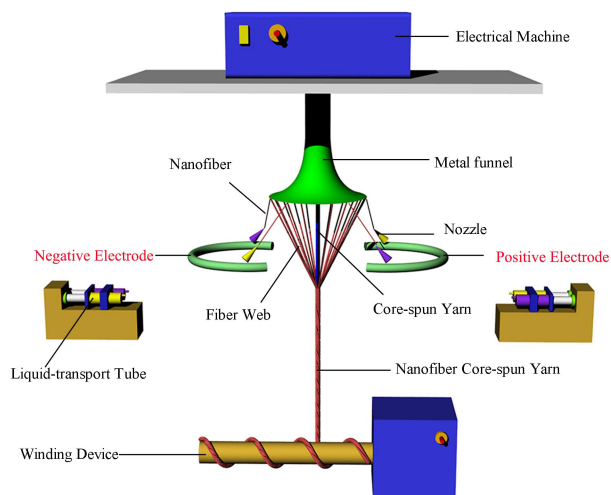


Figure S4 Schematic of double-conjugate electrospinning device for preparing nanofiber core-spun yarns.

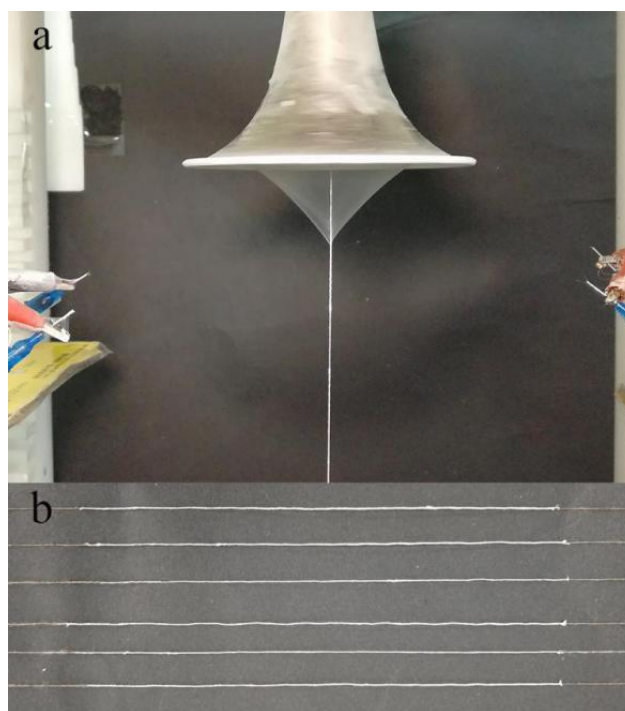


Figure S5 (a) Experimental images of nanofiber core-spun yarn based on Ni-coated cotton yarn as core yarn fabricated by double-conjugate electrospinning. (b) production of nanofiber core-spun yarn

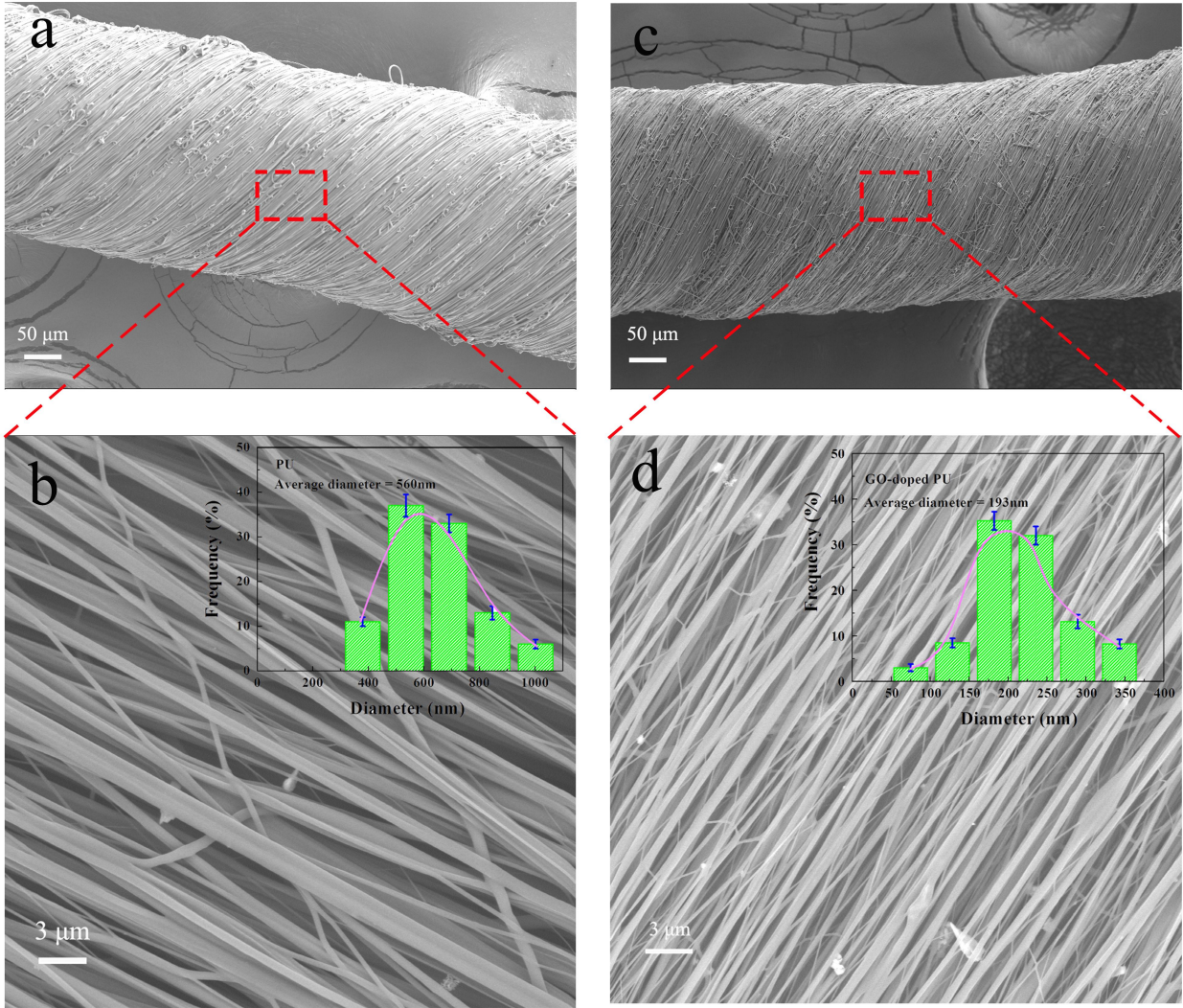


Figure S6 The low and high magnification SEM micrographs and diameter distribution histograms of (a, b) PU, (c, d) GO-doped PU nanofibers.

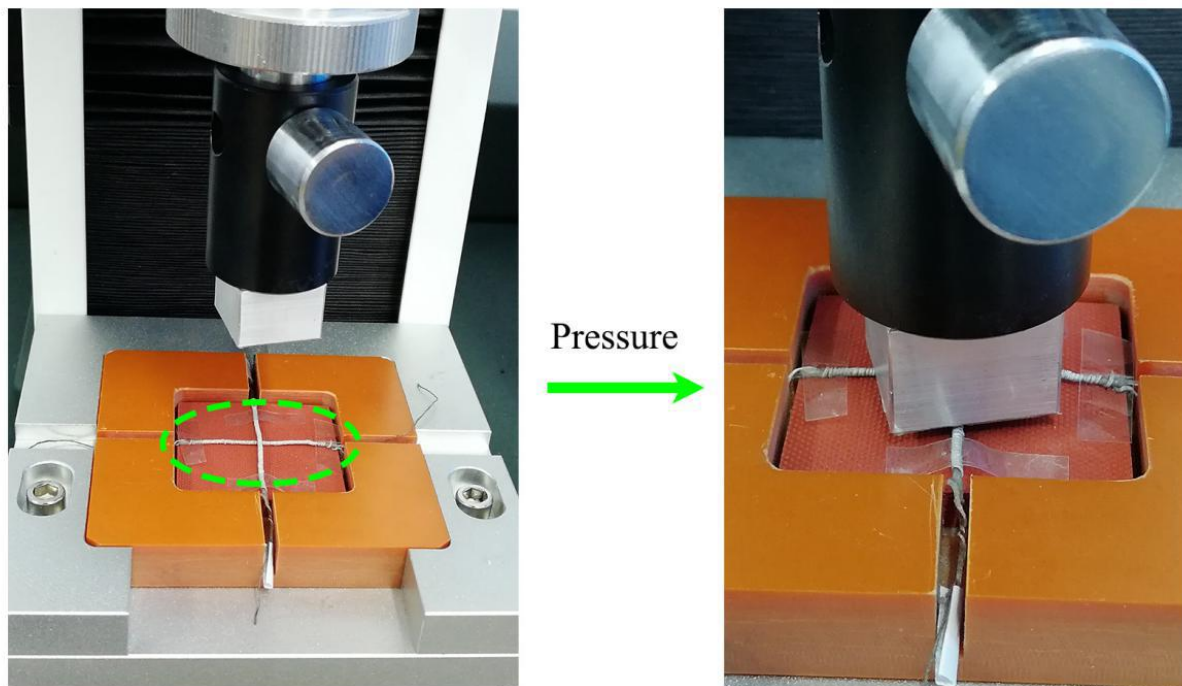


Figure S7 Photographs of a sensor unit during loading of loading force.

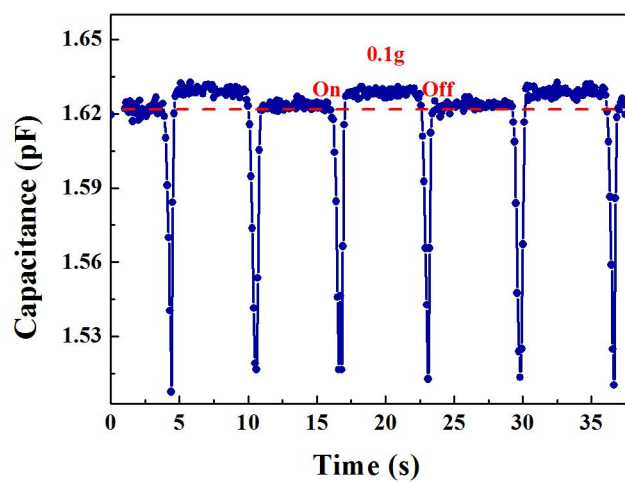


Figure S8 Transient response to the application and removal of a paper on the sensor unit, corresponding to a force of only 0.1g.

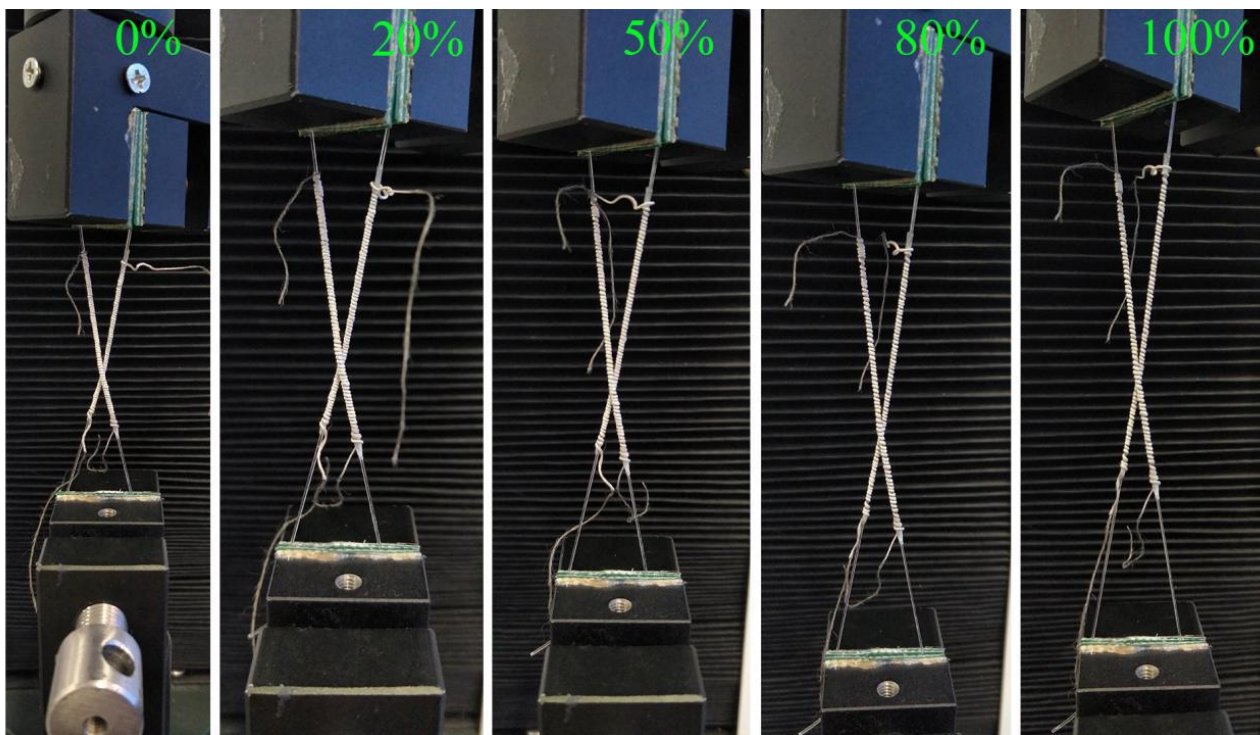


Figure S9 Photographs of a sensor unit during loading of increasing strain.

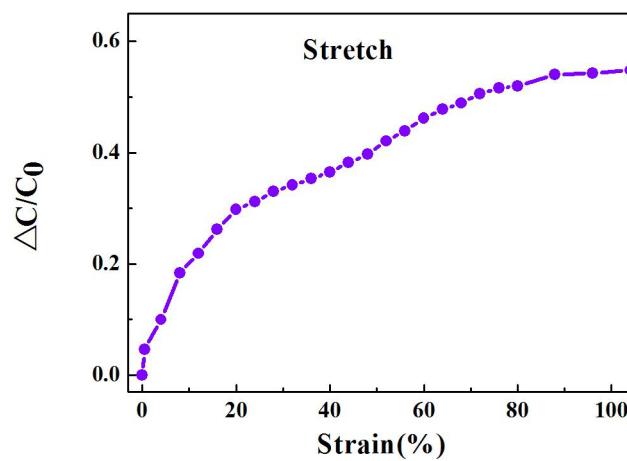


Figure S10 A non-linear change in capacitance depending on the different strains of the sensor unit based on GO-PNF/NiCY elastic composite yarn.

1-3 the capacitance of the sensor unit

$$\text{Strain} = (L_1 - L_0) / L_0$$

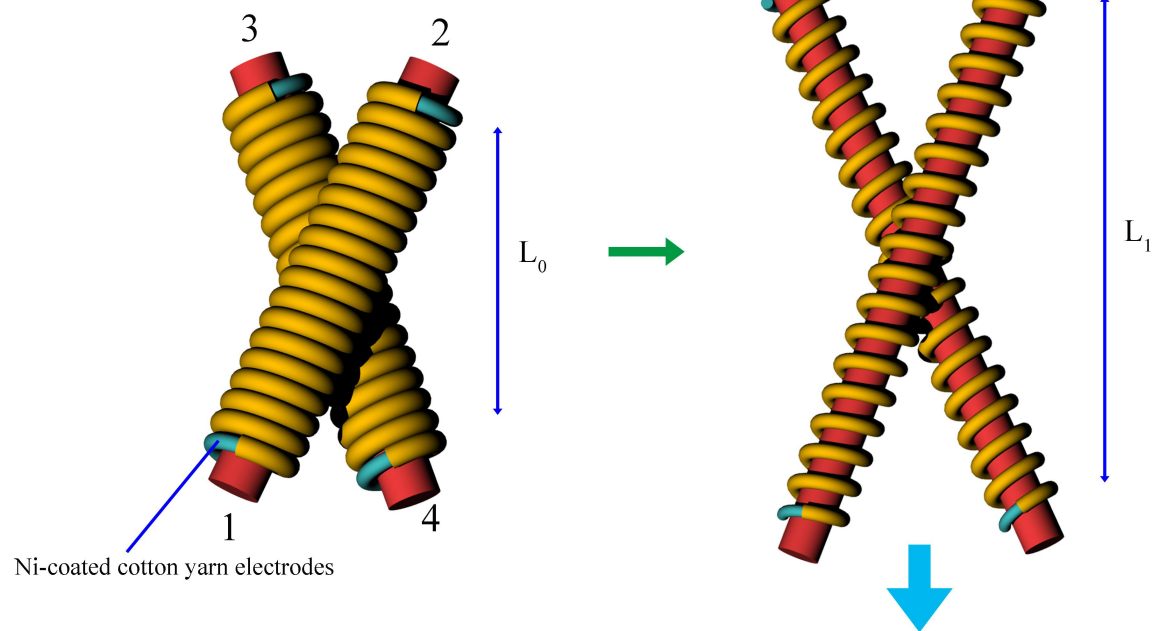


Figure S11 Stretch sensing mechanisms of the sensor unit. The capacitance change of the sensor unit (1-3) was measured by TH2829C meter.

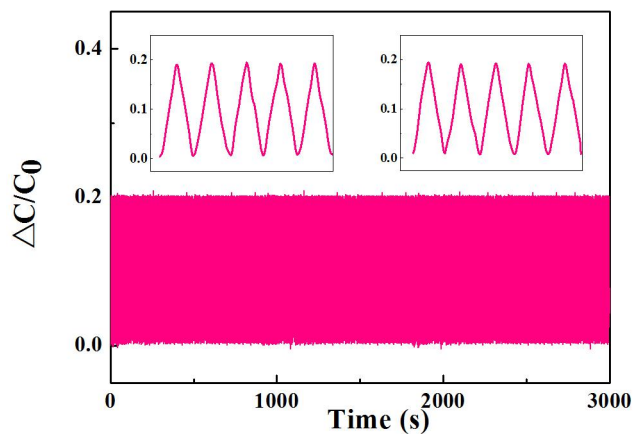


Figure S12 Performance of the sensor unit during 1,000 stretching-releasing cycles of a relatively small strain of 10%, indicating its remarkable stability and durability.

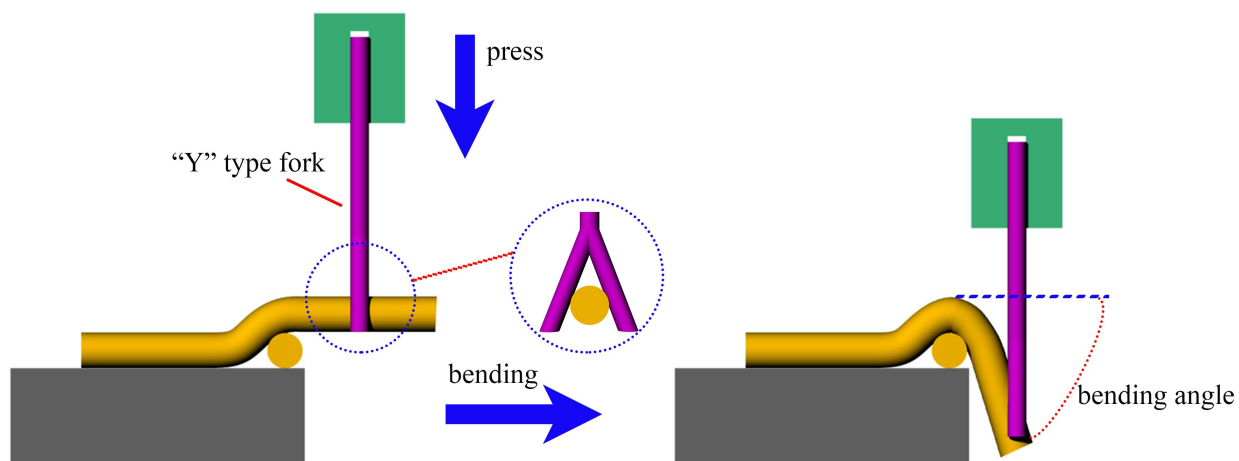


Figure S13 Schematic illustration of the test methods for the bending mechanical stimuli of the sensor unit.

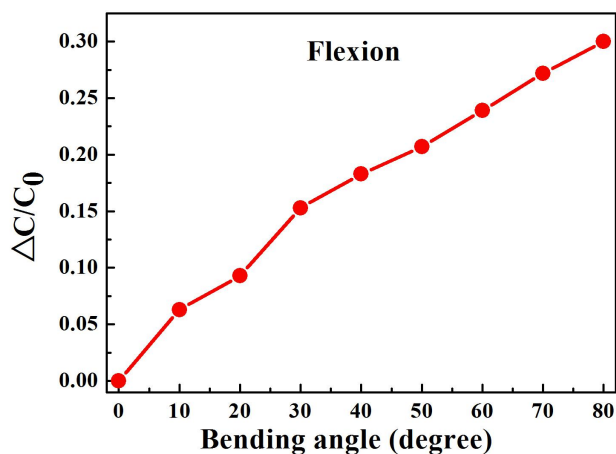


Figure S14 A linear change in capacitance depending on the different bending angle from 0 to 80° of the sensor unit based on GO-PNF/NiCY elastic composite yarn.

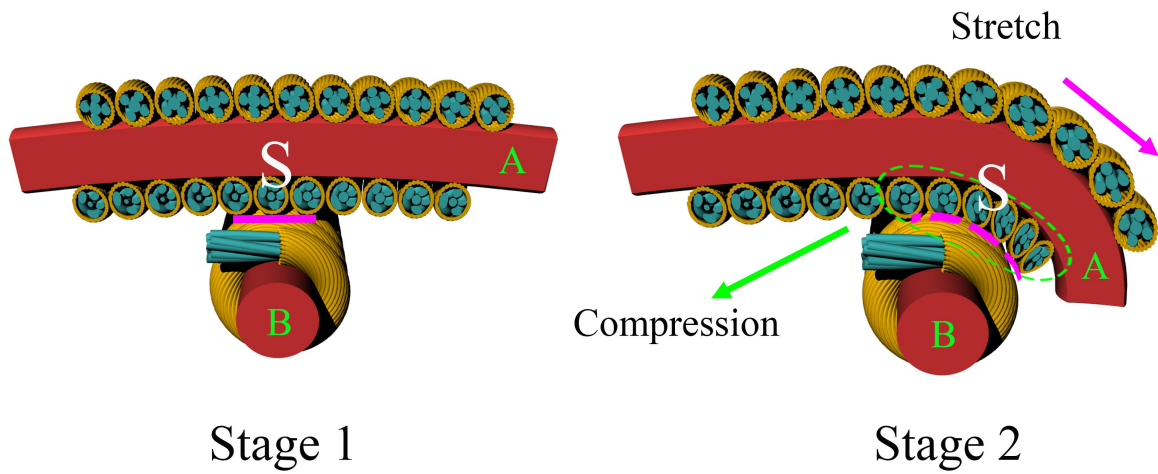


Figure S15 Bending sensing mechanisms of the sensor unit

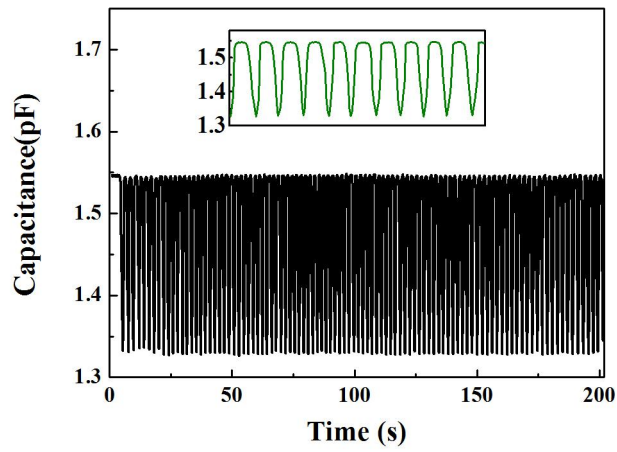


Figure S16 The capacitance response of the electronic fabric under 200 cycle tests when the fingers are close but not in contact

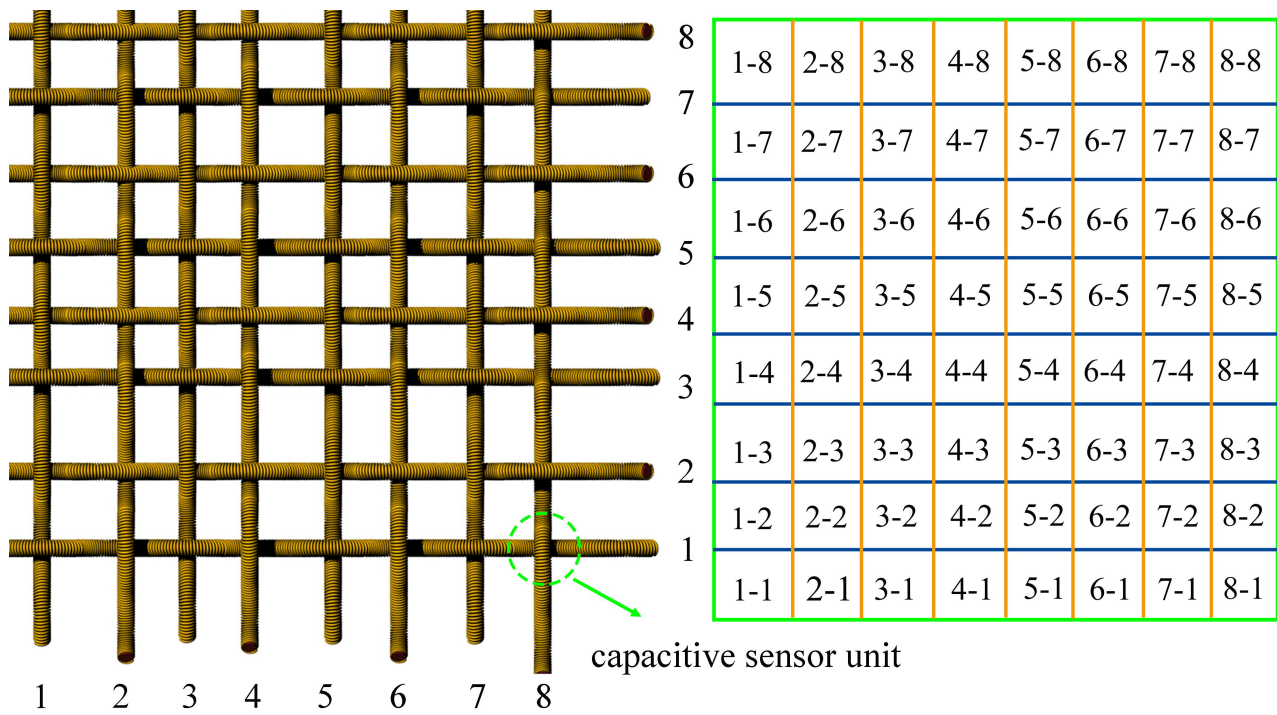


Figure S17 Schematic illustration of the data collected for 2D spatial mapping with the capacitance of each capacitive sensor unit. The capacitance of each row and column in the fabric are measured to draw 2D spatial mapping before and after the loading of mechanical force. For example “1-1” means the capacitance change of the sensor unit formed in the row 1 elastic composite yarn and column 1 elastic composite yarn.